COMMUNICATIONS IN NUMERICAL METHODS IN ENGINEERING
Commun. Numer. Meth. Engng 2007; **23**:71–84
Published online 19 June 2006 in Wiley InterScience (www.interscience.wiley.com). DOI: 10.1002/cnm.883

A lattice Boltzmann method for shock wave propagation in solids

Shaoping Xiao*, †, ‡

Department of Mechanical and Industrial Engineering and Center for Computer-Aided Design, The University of Iowa, U.S.A.

SUMMARY

This paper proposes a new lattice Boltzmann (LB) method for the study of shock wave propagation in elastic solids. The method, which implements a flux-corrected transport (FCT) algorithm, contains three stages: collision, streaming, and correction. In the collision stage, distribution functions are updated. In the streaming stage, the distribution functions are shifted between lattice points. Generally, a partial differential equation (PDE) is solved in the streaming stage, and finite element methods are employed to support the use of unstructured meshes in the LB method. The FCT algorithm is used in the correction stage to revise the distribution functions at lattice points, so fluctuations behind shock wave fronts can be eliminated efficiently. In this method, schemes for shock wave reflection at fixed and free boundaries are developed based on the bounce-back technique. A similar technique is used to treat wave reflection and transmission at material interfaces of composites. Several one-dimensional examples show that this LB-FCT method can provide ideal depictions of shock wave propagation in structures, especially composite structures.

Received 9 July 2005; Revised 31 March 2006; Accepted 24 April 2006

KEY WORDS: lattice Boltzmann method; flux-corrected transport; shock waves

1. INTRODUCTION

Some failure patterns of structures under dynamic loads, including spall fractures, radial fractures, and corner fractures, are due to shock wave interactions. Therefore, studies of shock wave propagation in solids will help us to understand the mechanisms of material failures under conditions of high pressure, velocity, and/or temperature as well as within very brief time intervals [1–3]. Numerical simulation has become a potential tool to explain such failure mechanisms [3–5]. However, most numerical methods experience difficulties in simulating shock wave propagation problems, since

*Correspondence to: Shaoping Xiao, 3131 Seamans Center, The University of Iowa, Iowa City, IA 52242, U.S.A.
†E-mail: shaoping-xiao@uiowa.edu
‡Assistant Professor.

Contract/grant sponsor: College of Engineering and Center for Computer-Aided Design (CCAD)

oscillations are always observed behind shock wave fronts. Therefore, non-oscillatory methods for shock wave propagation studies are always appealing.

Recently, lattice Boltzmann (LB) methods are of interest concerning the simulations of complex phenomena in hydrodynamics [6, 7], physics [8], mathematics [9], and chemistry [10]. The LB method, which was deeply rooted in the cellular automata (CA) modelling approach [11], contains two stages: collision and streaming. Particle distribution functions are updated in the collision stage, and they are shifted between lattice points in the streaming stage. Several LB models were developed with various approximations. Higuera *et al.* [12] enhanced the collision stage with the linearization of a collision operator. Xi and his coworkers proposed a discrete Boltzmann equation method [13, 14], which was based on the discretization of the Boltzmann equation [15] in space and time using the finite volume method. The finite difference method also was used for the disretization of the Boltzmann equation [16, 17]. Extensive research has been performed on the treatment of initial and boundary conditions [18–21]; however, the conventional LB methods require uniform meshes and encounter some difficulties with the problems involving complex geometries. He and his coworkers [22] made some progresses using LB methods, so the Navier–Stokes equation can be simulated on nonuniform mesh grids. Lee and Lin [23, 24] implemented a finite element method based on characteristics of the Galerkin method into LB methods for unstructured meshes.

LB methods have been used successfully in the field of computational fluid dynamics. It is of interest to extend such methods to solid mechanics. LB methods have been applied to simulate fluid–particle or fluid–structure interactions [8, 25–29]. In a solid body, the dynamics of the forces were illustrated using a LB formulation of a wave process, since elastic deformations in a solid propagate as waves. Chopard and Luthi [8] used an LB method to study fracture phenomena and obtained quality results. Since LB equations are derived from wave equations, LB methods have potential to study the shock wave propagation in solids. Most numerical methods, including finite element methods [30], have trouble catching shock wave fronts, because fluctuations are always observed behind wave fronts. Such phenomenon also can be seen when LB methods are used. One common technique used to reduce fluctuations behind shock wave fronts is the artificial bulk viscosity [31]. It can efficiently eliminate fluctuations, but shock wave fronts are observed to be spread over several elements or space step sizes. Moreover, the total energy of the system somewhat dissipates due to the artificial bulk viscosity. Studies have shown that the flux-corrected transport (FCT) algorithm can perfectly solve the issues mentioned above. Boris and Book first proposed the FCT algorithm [32, 33] in the 1970s. This algorithm consists of two stages: a transport stage and an antidiffusion stage. The antidiffusion stage is a corrective stage, which corrects numerical errors introduced in the transport stage. Both stages are conservative and positive. Their interaction enables the FCT algorithm to treat discontinuities without the usual dispersively generated ripples (oscillations). The FCT algorithm has been applied in different schemes of finite difference methods [33], and satisfactory results were obtained for shock test problems [32] in fluids. Moreover, implementations of the FCT algorithm in finite element methods have been conducted by Zhang *et al.* [34] and Xiao [35].

We develop a new LB method, which implements the FCT algorithm, in this paper to simulate shock wave propagation problems in solids. The macroscopic quantity related to the microscopic distribution functions is velocity in this method, and the Boltzmann equation is modified for solid mechanics. Different initial and nonzero prescribed boundary conditions are treated. The techniques based on the bounce-back schemes are modified to treat free boundaries, fixed boundaries, and material interfaces for shock wave reflection and transmission. The new LB method contains three stages: collision, streaming, and correction. After distribution functions are updated in the collision

DOI: 10.1002/cnm

stage, they are shifted between lattice points in the streaming stage. Finite element methods can be used in the streaming stage. Then, the distribution functions will be corrected using the FCT algorithm in the correction stage.

The outline of this paper is as follows: A new LB method for shock wave propagation in solids is proposed in Section 2. The treatments of initial and nonzero prescribed boundary conditions are described as well as wave reflections and transmissions on free boundaries, fixed boundaries, and material interfaces. Finite element methods are introduced to solve the PDE in the streaming stage in Section 3. In Section 4, an FCT algorithm is implemented to correct distribution functions at lattice points so that fluctuations behind shock wave fronts can be eliminated. Several one-dimensional examples are studied in Section 5 to show the advantages of the proposed LB method. The conclusions follow.

2. LB METHOD FOR ELASTIC SOLIDS

2.1. LB method

In an LB method, a particle distribution function $f_i(\mathbf{x}, t)$ is defined at each lattice point $\mathbf{x}$ and each discrete time t. The index i is associated with a lattice direction $\mathbf{c}_i$. For example, in a two-dimensional square lattice, $i = 1$ labels the right direction $\mathbf{c}_1 = (1, 0)$, $i = 2$ labels the up direction $\mathbf{c}_2 = (0, 1)$, and so on. The discrete Boltzmann equation is written as:

$$\frac{Df_i}{Dt} = -\frac{1}{\tau}(f_i - f_i^{(0)}) \tag{1}$$

where $D/Dt = (\partial/\partial t) + \mathbf{e}_i \cdot \nabla$ is the Lagrangian derivative along characteristics; $\mathbf{e}_i$ is the discrete microscopic velocity; τ is the relaxation parameter of collision; and $f_i^{(0)}$ is the equilibrium distribution function.

Generally, in LB methods for the Navier–Stokes equation, macroscopic quantities, the density ψ, and the momentum $\mathbf{J}$ can be defined via the standard procedure of statistical mechanics [36] as

$$\psi = \rho = \sum_i f_i, \qquad \mathbf{J} = \rho \mathbf{v} = \sum_i f_i \mathbf{e}_i \tag{2}$$

A new LB method is developed to solve solid mechanics problems in this paper with some modifications based on Reference [27]. Here, $\tau = 1/2$, which ensures reversibility, and the microscopic velocity $\mathbf{e}_i$ is defined as

$$\mathbf{e}_i = C\mathbf{c}_i = \mathbf{c}_i \sqrt{\frac{E}{\rho}} \tag{3}$$

where C is the wave speed; E is the Young's modulus; and ρ is the density. The macroscopic quantity $\boldsymbol{\psi}$ is defined as the velocity, i.e. $\boldsymbol{\psi}(\mathbf{x}, t) = \mathbf{v}(\mathbf{x}, t) = \sum_i \mathbf{f}_i(\mathbf{x}, t)$. $\boldsymbol{\psi}(\mathbf{x}, t)$ and its corresponding microscopic distribution functions, $\mathbf{f}_i(\mathbf{x}, t)$, are vectors in multidimensional problems, so $\boldsymbol{\psi} = \{\psi_x, \psi_y, \psi_z\}$ and $\mathbf{f}_i = \{f_{ix}, f_{iy}, f_{iz}\}$. Since the microscopic velocity $\mathbf{e}_i$ coincides with the wave speed, there are no rest fields $\mathbf{f}_0(\mathbf{x}, t)$. The equilibrium distribution function is defined as

$$f_{i\alpha}^{(0)}(\mathbf{x}, t) = \frac{1}{D}\psi_\alpha(\mathbf{x}, t) + \frac{1}{2}\mathbf{c}_i \cdot \mathbf{J}_\alpha(\mathbf{x}, t) \tag{4}$$

DOI: 10.1002/cnm

where D is the dimension of the microscopic velocity $\mathbf{e}_i$, and $\mathbf{J}_\alpha(\mathbf{x}, t) = \sum_i \mathbf{c}_i f_{i\alpha}(\mathbf{x}, t)$. Equation (1) can be used to obtain distribution functions at the time t_{n+1} if the distribution functions at the time t_n are known:

$$\mathbf{f}_i(\mathbf{x}(t_n) + \mathbf{e}_i \Delta t, t_{n+1}) = \mathbf{f}_i(\mathbf{x}(t_n), t_n) - \frac{\Delta t}{\tau}[\mathbf{f}_i(\mathbf{x}(t_n), t_n) - \mathbf{f}_i^{(0)}(\mathbf{x}(t_n), t_n)] \tag{5}$$

When Eulerian description [24] is used, Equation (1) or (5) can be expressed in a two-stage framework:

- *Collision*:

$$\mathbf{f}_i(\mathbf{x}, t_n) = \mathbf{f}_i(\mathbf{x}, t_n) - \frac{\Delta t}{\tau}[\mathbf{f}_i(\mathbf{x}, t_n) - \mathbf{f}_i^{(0)}(\mathbf{x}, t_n)] \tag{6}$$

- *Streaming*:

$$\mathbf{f}_i(\mathbf{x} + C\mathbf{c}_i \Delta t, t_{n+1}) = \mathbf{f}_i(\mathbf{x}, t_n) \tag{7}$$

Generally, the streaming stage can be written to solve the following PDE:

$$\frac{\partial \mathbf{f}_i}{\partial t} + \mathbf{e}_i \cdot \nabla \mathbf{f}_i = 0 \tag{8}$$

Equation (7) requires that the distance between two adjacent lattice points, Δx, is the distance that a wave travels during one time step Δt, i.e. $\Delta x = C\Delta t$, in each dimension. This distance is called the critical distance here, and it is denoted by Δx_c. If $\Delta x < \Delta x_c$, numerical simulations will be unstable due to the Courant condition. Equation (8) can be simplified to Equation (7) if the critical distance and the upwind finite difference method are used. In this paper, we only focus on one-dimensional problems, so Equation (8) can be written as

$$\frac{\partial f_i}{\partial t} + C c_i \frac{\partial f_i}{\partial x} = 0 \tag{9}$$

where $c_1 = -1$ and $c_2 = 1$ denote left and right directions, respectively. Next, we will describe the treatments for initial conditions, boundary conditions, and material interfaces under one-dimensional situations. Such techniques can easily be applied to multidimensional problems.

2.2. Initial and boundary conditions

We consider a one-dimensional lattice (chain) as shown in Figure 1. The number of lattice points is N and the left and right boundary points are point 1 and point N. If an initial velocity v_0 is

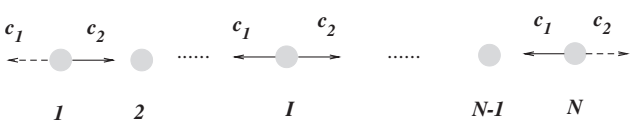

Figure 1. A one-dimensional lattice (chain).

DOI: 10.1002/cnm

applied on the lattice point I, the distribution functions of this lattice point at time $t=0$ can be set as

$$f_i(x_I,0)=\begin{cases} v_0, & i=2,\ I=1 \\ \frac{1}{2}v_0, & i=1,2,\ I\neq 1,N \\ v_0, & i=1,\ I=N \end{cases} \tag{10}$$

If an initial force F_0 or an initial displacement u_0 is applied, the corresponding initial velocities can be written as $v_0=(F_0/m_I)\Delta t$ or $v_0=u_0/\Delta t$, respectively, where m_I is the mass associated with the lattice point I. A similar formulation can be written for nonzero prescribed velocities $\bar{v}_1(t)$ and $\bar{v}_N(t)$, at boundary points:

$$f_2(x_1,t)=\bar{v}_1(t), \qquad f_1(x_N,t)=\bar{v}_N(t) \tag{11}$$

Bounce-back scheme [8] was used in most LB methods for fluid flows. However, the mechanisms of wave reflections on free boundaries and fixed boundaries are different in solids. The modified bounce-back scheme can be written as

$$f_2(x_1,t)=\lambda_1 f_1(x_1,t), \quad f_1(x_N,t)=\lambda_2 f_2(x_N,t) \tag{12}$$

where $\lambda_1=\lambda_2=1$ is for free boundary reflection, and $\lambda_1=\lambda_2=-1$ is for fixed boundary reflection. Distribution functions as shown by the direction of the dashed arrows in Figure 1 will be bounced back. After the streaming stage, the distribution function, $f_1(x_1,t)$, will be reflected to be $f_2(x_1,t)$ at boundary point 1, while $f_2(x_N,t)$ will be reflected to be $f_1(x_N,t)$ at boundary point N. The sign of the magnitude will be changed or kept the same according to boundary conditions. We know that when waves reach boundaries, velocities will be zero at fixed boundaries and double at free boundaries.

As a macroscopic quantity, the velocity is the summation of microscopic distribution functions, i.e. $v(x,t)=\psi(x,t)=f_1(x,t)+f_2(x,t)$. Therefore, Equation (12) exactly reproduces the physical phenomena observed when waves are reflected at boundaries. During numerical simulations, the modified bounce-back schemes are applied immediately after the streaming stage. The nonzero prescribed boundary conditions Equation (11) can be applied at the beginning of each time iteration.

2.3. Material interface

If waves propagate in a composite material, wave reflection and transmission can be observed at material interfaces as shown in Figure 2. When an incident wave in material A reaches a material interface Γ, part of the wave will be reflected and still propagate in material A. The rest of the wave will be transmitted through the interface and propagate in material B. Let ξ_{AB} denote the ratio of the acoustic impedance of material A to the one of material B. Then, it can be written as

$$\xi_{\mathrm{AB}}=(\rho_{\mathrm{A}}C_{\mathrm{A}})/(\rho_{\mathrm{B}}C_{\mathrm{B}})=\sqrt{E_{\mathrm{A}}\rho_{\mathrm{A}}}/\sqrt{E_{\mathrm{B}}\rho_{\mathrm{B}}} \tag{13}$$

Obviously, $\xi_{\mathrm{BA}}=\xi_{\mathrm{AB}}^{-1}$. The transmission and reflection coefficients for wave propagating from material A to B are denoted by $C_{\mathrm{AB}}^{\mathrm{T}}$ and $C_{\mathrm{AB}}^{\mathrm{R}}$, and they can be written as

$$C_{\mathrm{AB}}^{\mathrm{T}}=\frac{2}{1+\xi_{\mathrm{AB}}}, \quad C_{\mathrm{AB}}^{\mathrm{R}}=\frac{1-\xi_{\mathrm{AB}}}{1+\xi_{\mathrm{AB}}} \tag{14}$$

We can see that $C_{\mathrm{AB}}^{\mathrm{R}}+1=C_{\mathrm{AB}}^{\mathrm{T}}$ is satisfied.

DOI: 10.1002/cnm

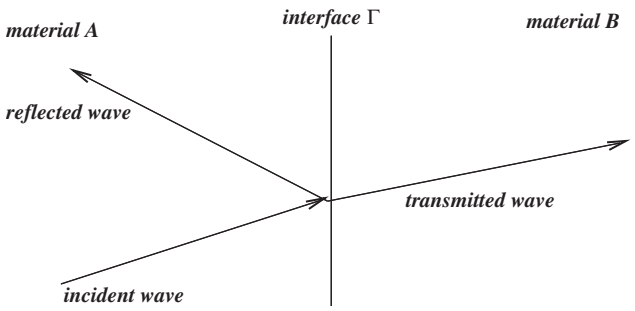

Figure 2. Wave reflection and transmission at a material interface.

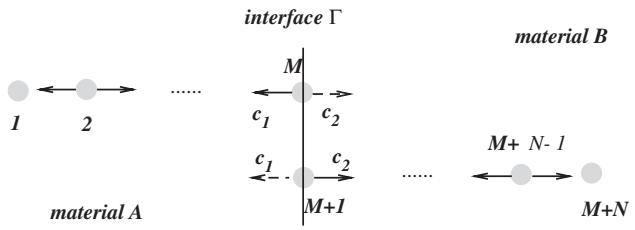

Figure 3. LB modelling of a material interface in one-dimensional lattice (chain).

An LB modelling of a material interface is shown in Figure 3 for a one-dimensional problem. There are M lattice points uniformly arranged in material A, and N lattice points in material B. Points M and $M+1$ are coincident at the material interface Γ. After the streaming stage, the distribution functions $f_2(x_M, t)$ at point M and $f_1(x_{M+1}, t)$ at point $M+1$ will be reflected and transmitted at the interface. The distribution function $f_2(x_{M+1}, t)$ of point $M+1$ is contributed by the transmission of $f_2(x_M, t)$ and the reflection of $f_1(x_{M+1}, t)$ based on the following rule:

$$f_2(x_{M+1}, t) = C^{\mathrm{T}}_{\mathrm{AB}} f_2(x_M, t) + C^{\mathrm{R}}_{\mathrm{BA}} f_1(x_{M+1}, t) \tag{15}$$

Similarly, the distribution function $f_1(x_M, t)$ at point M can be written as

$$f_1(x_M, t) = C^{\mathrm{T}}_{\mathrm{BA}} f_1(x_{M+1}, t) + C^{\mathrm{R}}_{\mathrm{AB}} f_2(x_M, t) \tag{16}$$

where $C^{\mathrm{T}}_{\mathrm{BA}}$ and $C^{\mathrm{R}}_{\mathrm{BA}}$ are the transmission and reflection coefficients when wave propagating from material B to material A. Finally, we allow $f_2(x_M, t) = f_2(x_{M+1}, t)$ and $f_1(x_{M+1}, t) = f_1(x_M, t)$ to enforce the compatibility between lattice points M and $M+1$.

In one-dimensional problems, if materials A and B have different areas of cross-section, A_{A} and A_{B}, the ratio of the acoustic impedances in Equation (13) can be written as

$$\xi_{\mathrm{AB}} = (\rho_{\mathrm{A}} C_{\mathrm{A}} A_{\mathrm{A}})/(\rho_{\mathrm{B}} C_{\mathrm{B}} A_{\mathrm{B}}) = \sqrt{E_{\mathrm{A}} \rho_{\mathrm{A}}} A_{\mathrm{A}} / \sqrt{E_{\mathrm{B}} \rho_{\mathrm{B}}} A_{\mathrm{B}} \tag{17}$$

DOI: 10.1002/cnm

3. FINITE ELEMENT METHODS IN THE STREAMING STAGE

The streaming stage is a key stage in LB methods. As mentioned before, the critical distance $\Delta x_c = C\Delta t$ does not have to be used as the distance between two adjacent lattice points. The general streaming stage is solving a PDE, as shown in Equation (9). Finite difference methods were widely used, but they require structured meshes. Unstructured meshes have more potential, especially for multidimensional problems. Therefore, finite element methods are introduced, so the proposed LB method can be applied to multidimensional problems with arbitrary geometries.

Generally, a Lax–Wendroff scheme [24] is used to approximate Equation (9), and it is:

$$\frac{f_i(x_n, t_{n+1}) - f_i(x_n, t_n)}{\Delta t} = -c_i C \frac{\partial f_i(x_n, t_n)}{\partial x} + \frac{\Delta t}{2} C^2 \frac{\partial^2 f_i(x_n, t_n)}{\partial x^2} \tag{18}$$

Equation (18) can be viewed as a continuous equation in space domain, and finite element methods can be used to solve it in the streaming stage. The lattice points are set on the vertices of the elements. The distribution function field can be approached using the finite element approximation

$$f_i^h(x, t_n) = \sum_I N_I(x) f_i(x_I, t_n) \tag{19}$$

where $N_I(x)$ are shape functions, and they reproduce constant functions and linear functions, i.e. $\sum_I N_I(x) = 1$ and $\sum_I (\partial N_I(x)/\partial x) x_I = 1$. The weak form of Equation (18) can be derived by using the Galerkin method:

$$\begin{aligned} &\int_\Omega w[f_i(x, t_{n+1}) - f_i(x, t_n)]\, \mathrm{d}\Omega \\ &= -c_i \Delta t C \int_\Omega w \frac{\partial f_i(x, t_n)}{\partial x}\, \mathrm{d}\Omega - \frac{\Delta t^2 C^2}{2} \left[\int_\Omega \frac{\partial w}{\partial x} \frac{\partial f_i(x, t_n)}{\partial x}\, \mathrm{d}\Omega \right. \\ &\quad \left. - \int_\Gamma w \frac{\partial f_i(x, t_n)}{\partial x} n_x\, \mathrm{d}\Gamma \right] \end{aligned} \tag{20}$$

where w is the weight function. Note that Green–Gauss theorem is used here. After substituting Equation (19) into Equation (20), an FE equation can be obtained:

$$\begin{aligned} &M_{IJ}[f_i(x_J, t_{n+1}) - f_i(x_J, t_n)] \\ &= -c_i \Delta t C K_{IJ}^\alpha f_i(x_J, t_n) - \frac{\Delta t^2 C^2}{2} (K_{IJ}^\beta - K_{IJ}^\gamma) f_i(x_J, t_{n+1}) \end{aligned} \tag{21}$$

where

$$M_{IJ} = \int_\Omega N_I(x) N_J(x)\, \mathrm{d}\Omega, \qquad K_{IJ}^\alpha = \int_\Omega N_I(x) \frac{\partial N_J(x)}{\partial x}\, \mathrm{d}\Omega \tag{22}$$

$$K_{IJ}^\beta = \int_\Omega \frac{\partial N_I(x)}{\partial x} \frac{\partial N_J(x)}{\partial x}\, \mathrm{d}\Omega, \quad K_{IJ}^\gamma = \int_\Gamma N_I(x) \frac{\partial N_J(x)}{\partial x} n_x\, \mathrm{d}\Gamma \tag{23}$$

DOI: 10.1002/cnm

For simplification, a lumped matrix is used to replace the consistent matrix M_{IJ}:

$$M_{IJ} = \delta_{IJ} \sum_K \int_\Omega N_I(x) N_K(x)\, \mathrm{d}\Omega \tag{24}$$

In fact, we borrow the lumped mass matrix idea, because the above matrix can be viewed as the mass matrix for the material with the density $\rho = 1$. Here, M_I is used to denote the diagonal components of the lumped matrix in Equation (24).

K_{IJ}^{γ} is produced by a surface integration where n_x is the normal direction of the surface, and it is -1 on the left boundary point and 1 on the right boundary point in one-dimension problems. Therefore, in the streaming step the following equation will be solved to shift distribution functions at lattice points:

$$f_i(x_I, t_{n+1}) = f_i(x_I, t_n) - \frac{\Delta t C}{M_I}\left[c_i K_{IJ}^{\alpha} + \frac{\Delta t C}{2}(K_{IJ}^{\beta} - K_{IJ}^{\gamma})\right] f_i(x_J, t_n) \tag{25}$$

Once distribution functions are shifted in the streaming stage, the motion of lattice points and strain/stress fields can be obtained as

$$v(x_I, t) = \psi(x_I, t) = f_1(x_I, t) + f_2(x_I, t) \tag{26}$$

$$u(x_I, t) = v(x_I, t)\Delta t \tag{27}$$

$$\varepsilon(x, t) = \frac{\partial u(x, t)}{\partial x} = \sum_I \frac{\partial N_I(x)}{\partial x} u(x_I, t) \tag{28}$$

$$\sigma(x, t) = E\varepsilon(x, t) \tag{29}$$

where $u(x_I, t)$ is the displacement of point I; ε is the uniaxial strain; and σ is the uniaxial stress.

4. IMPLEMENTATION OF THE FCT ALGORITHM

The FCT algorithm was first used in finite difference methods [32, 33]. Some researchers have implemented it into finite element methods [34, 35] once differential equations are in need of solving and discontinuities are in need of treatment. It can also be implemented into the LB method to assist us in simulating shock wave propagations in solids.

Since Equation (9) is the only PDE solved in the streaming stage, the FCT algorithm can be applied after each streaming step to correct distribution functions at lattice points. The flowchart for the FCT algorithm in the proposed LB method can be written as follows after trial distribution functions, $\tilde{f}_i(x_I, t_{n+1})$, are obtained from solving Equation (9) using finite element method.

(a) *Calculate the diffusive fluxes*:

$$\varphi_{iI}^0 = \eta_1(f_i(x_{I+c_i}, t_n) - f_i(x_I, t_n)) \tag{30}$$

(b) *Diffusion*:

$$\bar{f}_i(x_I, t_{n+1}) = \tilde{f}_i(x_I, t_{n+1}) + \varphi_{iI}^0 - \varphi_{iI-c_i}^0 \tag{31}$$

DOI: 10.1002/cnm

(c) *Calculate antidiffusive fluxes*:

$$\varphi_{iI}^{1} = \eta_2(\tilde{f}_i(x_{I+c_i}, t_{n+1}) - \tilde{f}_i(x_I, t_{n+1})) \tag{32}$$

(d) *Apply limitation of antidiffusive fluxes*:

$$\varphi_{iI}^{C} = S \cdot \max\{0, \min[S \cdot \Delta_{iI-1}, |\varphi_{iI}^{1}|, S \cdot \Delta_{iI+1}]\} \tag{33}$$

where $\Delta_{iI} = \bar{f}_i(x_{I+c_i}, t_{n+1}) - \bar{f}_i(x_I, t_{n+1})$, and $S = \text{sign}(\varphi_{iI}^{1})$.

(e) *Antidiffusion*:

$$f_i(x_I, t_{n+1}) = \bar{f}_i(x_I, t_{n+1}) - \varphi_{iI}^{C} + \varphi_{iI-c_i}^{C} \tag{34}$$

Note c_i is used in the subscripts of x, since there are two directions for distribution functions at each lattice point. Therefore, the new LB method for shock wave propagation in solids contains three stages:

- *Collision*:

$$f_i(x, t_n) = f_i(x, t_n) - 2\Delta t[f_i(x, t_n) - f_i^{(0)}(x, t_n)] \tag{35}$$

- *Streaming*: using the FD method, the FE method, or the MP method to shift f_i

$$\frac{\partial f_i}{\partial t} + e_i \frac{\partial f_i}{\partial x} = 0 \tag{36}$$

- *Correction*: using the FCT algorithm to correct f_i.

In this paper, the diffusive and antidiffusive coefficients are constant, i.e. $\eta_1 = \eta_2 = 0.125$ [32, 33].

5. EXAMPLES

Shock wave propagation in a one-dimensional elastic rod will be studied in the following examples with various initial and boundary conditions. In most cases, the material properties are given as follows without notice: the length $L = 1$ m, the density $\rho = 100\ \text{kg/m}^3$, the area of cross-section of the rod $A = 1\ \text{m}^2$, and the Young's modulus $E = 10^6\ \text{N/m}^2$. Therefore, the wave speed in this elastic rod is $C = \sqrt{E/\rho} = 100\ \text{m/s}$. The time step used in this paper is 5×10^{-6} s, so the critical space size is $\Delta x_c = C\Delta t = 5 \times 10^{-4}$ m. The lattice spacing should be larger than or equal to the critical space size for stable numerical simulations.

5.1. Dynamic loads applied on one end

A dynamic load (force) is applied on the left end of the rod, as shown in Figure 4 where $f_0 = 10\,000$ N, and $t_0 = 4 \times 10^{-3}$ s. Then, then prescribed boundary condition is

$$f_2(x_1, t) = \frac{f_0 \Delta t}{m_1}, \quad t < t_0 \tag{37}$$

A 1001 lattice points are used in this example. Figure 5 shows the perfect evolutions of shock waves at $t_1 = 5 \times 10^{-3}$ s, $t_2 = 1.3 \times 10^{-2}$ s and $t_3 = 1.8 \times 10^{-2}$ s. There is a stress wave propagating

DOI: 10.1002/cnm

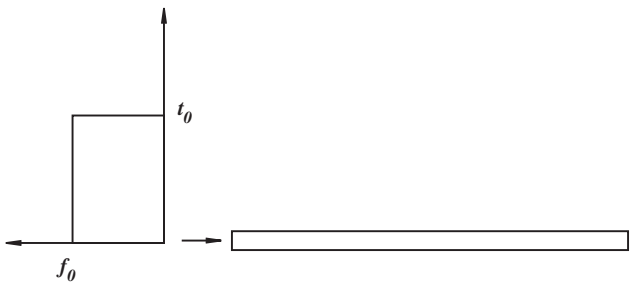

Figure 4. A dynamic load is applied on the left end of the rod whose right end is free.

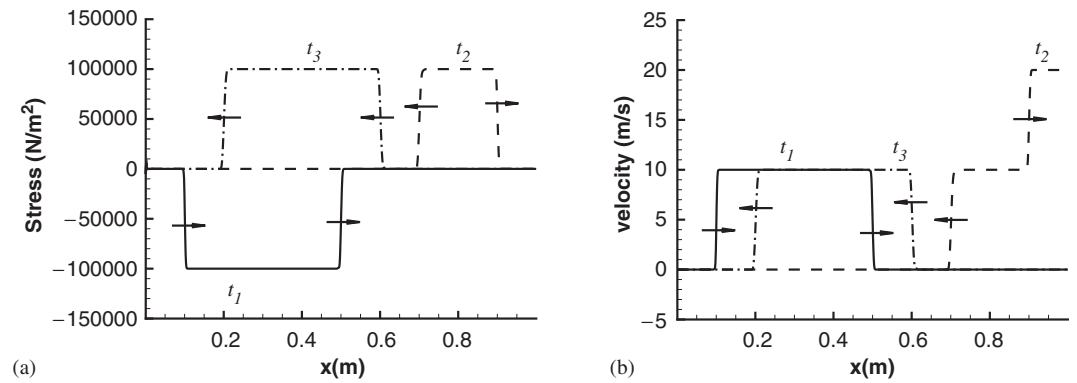

Figure 5. Evolutions of shock waves: (a) stress; and (b) velocity.

after the initial force loads. It is a compressive stress wave (the magnitude is negative here) as shown in Figure 5(a). Since the right end of the rod is free, the compressive stress shock wave becomes a tensile stress shock wave after reflection. We know that the mechanism of velocity wave propagation is different from stress wave propagation. In Figure 5(b), we can see that the magnitude of the velocity wave keeps the same sign after the reflection at the free boundary.

5.2. Shock wave propagation in a composite rod

An elastic composite rod is loaded by a velocity pulse as shown in Figure 6, where $v_0 = 10\,\mathrm{m/s}$ and $t_0 = 2.5 \times 10^{-3}\,\mathrm{s}$. Material A has the same material properties as we used before. The Young's modulus of the material B is $E_\mathrm{B} = 6.4 \times 10^5\,\mathrm{N/m^2}$, and the density is $\rho_\mathrm{B} = \rho_\mathrm{A} = 100\,\mathrm{kg/m^3}$. Therefore, the ratio of the acoustic impedances of material A to material B is $\xi_{\mathrm{AB}} = \sqrt{E_\mathrm{A}/E_\mathrm{B}} = 1.25$. The transmission and reflection coefficients from material A to material B can be calculated according to Equation (14):

$$C_{\mathrm{AB}}^{\mathrm{R}} = \frac{1 - \xi_{\mathrm{AB}}}{1 + \xi_{\mathrm{AB}}} = -0.11, \quad C_{\mathrm{AB}}^{\mathrm{T}} = \frac{2}{1 + \xi_{\mathrm{AB}}} = 0.89 \tag{38}$$

DOI: 10.1002/cnm

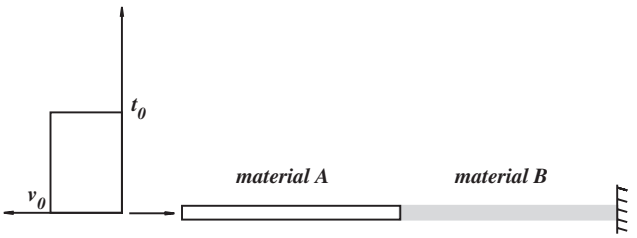

Figure 6. An elastic composite rod loaded by a velocity pulse.

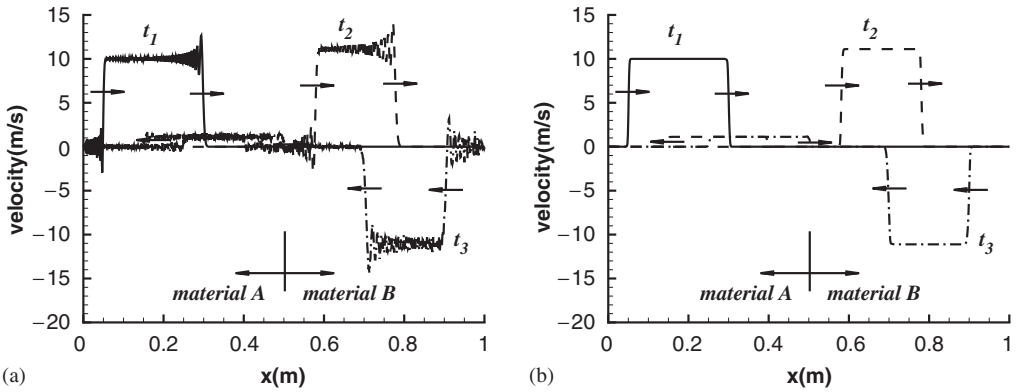

Figure 7. Evolution of the shock wave in an elastic composite rod: (a) conventional finite element simulation; and (b) LB simulation with the FCT algorithm.

When the shock wave reaches the material interface, part of it will be reflected back and the rest will transmit at the material interface. Figure 7 shows the evolution of shock waves in this elastic composite rod at $t_1 = 2.5 \times 10^{-3}$ s, $t_2 = 8.5 \times 10^{-3}$ s and $t_3 = 1.5 \times 10^{-2}$ s. The results from the conventional finite element simulation are shown in Figure 7(a). It is difficult to decipher the reflected shock wave due to the oscillations behind shock wave fronts. However, the LB method with the FCT algorithm provides perfect results, as shown in Figure 7(b).

5.3. Shock wave propagation in the elastic rod with various areas of cross-section

Figure 8 shows that an elastic composite rod with various areas of cross-section under the prescribed velocity pulses on both ends, $v_0 = 10$ m/s and $t_0 = 2.5 \times 10^{-3}$ s. The properties of material A to B are the same as the previous example. The areas of the cross-section are $A_A = 1.0\ \text{m}^2$ and $A_B = 2.0\ \text{m}^2$ for material A and B, respectively. The ratio of acoustic impedances of material A to B is $\xi_{AB} = 0.625$, so the reflection and transmission coefficients are $C_{AB}^R = 0.23$ and $C_{AB}^T = 1.23$. The evolution of shock waves at $t_1 = 3.5 \times 10^{-3}$ s and $t_2 = 9 \times 10^{-3}$ s is shown in Figure 9. When the waves start to propagate in the rod, two waves propagate with different wave speeds and wave lengths in different materials. Both of the waves will be reflected and transmitted at the material

DOI: 10.1002/cnm

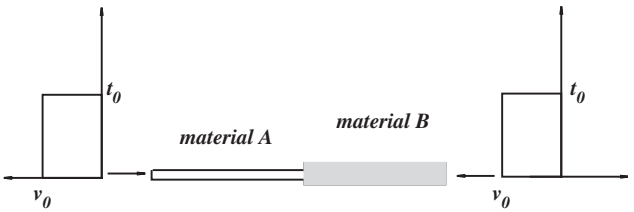

Figure 8. An elastic rod with various area of cross-section.

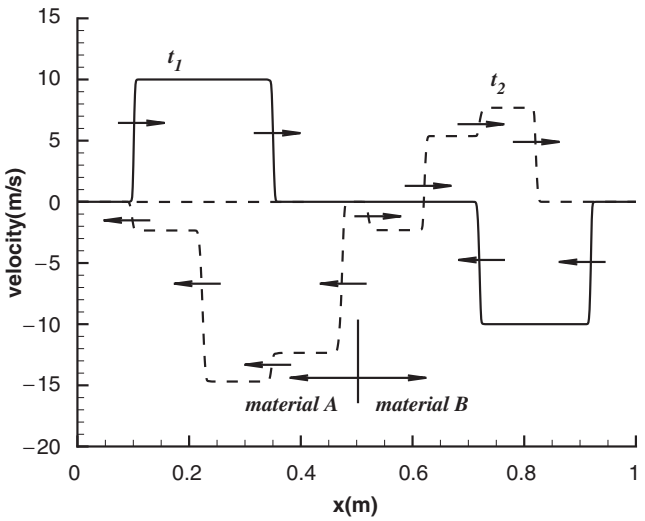

Figure 9. Evolution of shock waves in an elastic composite rod with various areas of cross-sections.

interfaces, and the waves interact when they meet with each other. Similar to what is shown in Figure 7(a) it will be hard to decipher wave interaction due to fluctuations behind shock wave fronts. From Figure 9, we can say that the proposed LB method is an ideal method to study the interactions of shock waves.

6. CONCLUSIONS

A new LB modelling for shock wave propagation in solids is developed in this paper. After updating distribution functions at the collision stage, finite element methods are used to solve a general PDE at the streaming stage for distribution functions' shifting between lattice points. The use of finite element methods at the streaming stage results in the potential of the LB method for solving multidimensional problems with unstructured meshes. A new stage, the correction stage, is added following the streaming stage. In this stage, the FCT algorithm is implemented to correct

DOI: 10.1002/cnm

distribution functions at lattice points, so fluctuations behind shock wave fronts can be efficiently eliminated. Another feature of this LB modelling is that the bounce-back scheme is modified for various boundary conditions as well as material interfaces. The examples show that the new LB method can accurately describe the shock wave propagation in solids, including reflection at boundaries, reflection and transmission at material interfaces, and interaction between shock waves. Even though this paper primarily focuses on one-dimensional problems in this paper, the proposed LB method has potential to be extended for multidimensional problems. This LB method is also suitable to study failure patterns of structures, especially composite structures, under dynamics loads.

ACKNOWLEDGEMENTS

The author gratefully acknowledges the startup fund support contributed by the College of Engineering and Center for Computer-Aided Design (CCAD) of the University of Iowa. The author is also very thankful for fruitful discussion with University of Iowa Professor Ching-Long Lin of the Department of Mechanical and Industrial Engineering and IIHR—Hydroscience and Engineering.

REFERENCES

1. Batkov YV, Novikov SA, Chernov AV. Shear-strength of solids and its effect on plane shock-wave propagation. *Combustion Explosion and Shock Waves* 1986; **22**:238–244.
2. Shen AH, Anrens TJ, O'Keefe JD. Shock wave induced vaporization of porous solids. *Journal of Applied Physics* 2003; **93**:5167–5174.
3. Mabssout M, Pastor M. A Taylor–Galerkin algorithm for shock wave propagation and strain localization failure of viscoplastic continua. *Computer Methods in Applied Mechanics and Engineering* 2003; **192**:955–971.
4. Lomov I, Rubin MB. Numerical simulation of damage using an elastic-viscoplastic model with directional tensile failure. *Journal of Physics IV* 2003; **110**:281–286.
5. Volkov IA. Numerical investigation of the spall failure of copper by shock-wave loading. *Combustion Explosion and Shock Waves* 1992; **28**:93–100.
6. Flekkoy E, Herrmann H. Lattice Boltzmann models for complex fluids. *Physica A* 1993; **199**:1–11.
7. Chen S, Doolen GD. Lattice Boltzmann method for fluid flows. *Annual Review of Fluid Mechanics* 1998; **30**:329–364.
8. Chopard B, Luthi PO. Lattice Boltzmann computations and applications to physics. *Theoretical Computer Science* 1999; **217**:115–130.
9. Brosilow BJ, Ford RM, Sarman S, Cummings PT. Numerical solution of transport equations for bacterial chemotaxis: effect of discretization of directional motion. *SIAM Journal on Applied Mathematics* 1996; **56**: 1639–1663.
10. Chen S, Dawson SP, Doolen GD, Janecky DR, Lawniczak A. Lattice methods and their applications to reacting systems. *Computers and Chemical Engineering* 1995; **19**:617–646.
11. Chopard B. A cellular automata model of large scale moving objects. *Journal of Physics A* 1990; **23**:1671–1687.
12. Higuera FJ, Succi S, Benzi R. Lattice gas-dynamics with enhanced collision. *Europhysics Letters* 1989; **9**:345–349.
13. Xi H, Peng G, Chou SH. Finite-volume lattice Boltzmann method. *Physical Review E* 1999; **59**:6202–6205.
14. Xi H, Peng G, Chou SH. Finite-volume lattice Boltzmann schemes in two and three dimensions. *Physical Review E* 1999; **60**:3380–3388.
15. Wolf-Gladrow D. *Lattice-Gas Cellular Automata and Lattice Boltzmann Models*. Springer: Heidelberg, 2000.
16. Guo ZL, Zhao TA. Explicit finite-difference lattice Boltzmann method for curvilinear coordinates. *Physical Review E* 2003; **67**:066709.
17. Mei R, Shyy W. On the finite difference-based lattice Boltzmann method in curvilinear coordinates. *Journal of Computational Physics* 1998; **143**:426–448.
18. D'Orazio A, Succi S. Boundary conditions for thermal lattice Boltzmann simulations. *Lecture Notes in Computer Science* 2003; **2657**:977–986.

DOI: 10.1002/cnm

19. Ansumali S, Karlin IV. Kinetic boundary conditions in the lattice Boltzmann method. *Physical Review E* 2002; **66**:026311.
20. Skordos PA. Initial and boundary conditions for the lattice Boltzmann method. *Physical Review E* 1993; **48**:4823–4842.
21. Chen S, Martinez D, Mei R. On boundary conditions in lattice Boltzmann methods. *Physics of Fluids* 1996; **8**:2527–2536.
22. He X, Luo LS, Dembo M. Some progress in lattice Boltzmann method. Part I. Nonuniform mesh grids. *Journal of Computational Physics* 1996; **129**:357–363.
23. Lee T, Lin C. A characteristic Galerkin method for discrete Boltzmann equation. *Journal of Computational Physics* 2001; **171**:336–356.
24. Lee T, Lin C. An Eulerian description of the streaming process in the lattice Boltzmann equation. *Journal of Computational Physics* 2003; **185**:445–471.
25. Feng ZG, Michaelides EE. The immersed boundary-lattice Boltzmann method for solving fluid–particles interaction problems. *Journal of Computational Physics* 2004; **195**:602–628.
26. Chopard B, Marconi S. Lattice Boltzmann solid particles in a lattice Boltzmann fluid. *Journal of Statistical Physics* 2002; **107**:23–37.
27. Marconi S, Chopard B. A lattice Boltzmann model for a solid body. *International Journal of Modern Physics B* 2003; **17**:153–156.
28. Heemels MW, Magen MHJ, Lowe CP. Simulating solid colloidal particles using the lattice-Boltzmann method. *Journal of Computational Physics* 2000; **164**:48–61.
29. Ladd AJC, Verberg R. Lattice-Boltzmann simulations of particle-fluid suspensions. *Journal of Statistical Physics* 2001; **104**:1191–1251.
30. Hughes TJR. *The Finite Element Method*: *Linear Static and Dynamic Analysis*. Prentice-Hall/Dover: Englewood Cliffs/New York, 1987.
31. Zukas JA. *High Velocity Impact Dynamics*. Wiley: New York, 1990.
32. Boris JP, Book DL. Flux-corrected transport 1. SHASTA, a fluid transport algorithm that works. *Journal of Computational Physics* 1973; **11**:38–69.
33. Boris JP, Book DL, Hain K. Flux-corrected transport 2. Generalizations of the method. *Journal of Computational Physics* 1975; **18**:248–283.
34. Zhang JH, Duan ZP, Ding J. Simulating shock to detonation transition: algorithm and results. *Journal of Computational Physics* 1999; **150**:128–142.
35. Xiao SP. A FE-FCT method with implicit functions for the study of shock wave propagation in solid. *Wave Motion* 2004; **40**:263–276.
36. Rėsibois P, Leener M. *Classical Kinetic Theory of Fluids*. Wiley: New York, 1977.

DOI: 10.1002/cnm